Строительные материалы и изделия
Construction Materials and Products

journal homepage: https://bstu-journals.ru

ISSN
2618-7183

DOI: 10.58224/2618-7183-2025-8-1-2

Photocatalysts based on Zn-Ti layered double hydroxide and its calcination products for self-cleaning concretes: Structure formation and photocatalytic activity

Balykov A.S. * [1], Nizina T.A. [1], Chugunov D.B. [1], Davydova N.S. [1], Kyashkin V.M. [1]

[1] National Research Mordovia State University, Russia

Abstract. Currently, the development of highly active photocatalytic additives for self-cleaning cement materials is a topical direction of building materials science. Mixed transition metal oxides are one of the effective types of photocatalysts, because they have improved functional characteristics compared to monometallic compounds. The purpose of this study was to establish the effects of synthesis conditions on the structure parameters and photocatalytic activity of zinc-titanium layered double hydroxide (Zn-Ti LDH) with Zn^{2+}/Ti^{4+} molar ratio of 2/1, as well as its calcination products in the form of zinc-titanium mixed metal oxides (Zn-Ti MMOs). It was found that the mixing temperature of solutions of precursor salts and precipitators, as well as the temperature of sediment aging, were the main synthesis parameters that had the greatest impact on the phase composition and crystallite size of layered double hydroxide.

The research results showed differences in the kinetics of photodestruction of methylene blue (MB) in solution under UV radiation in the presence of Zn-Ti layered double hydroxide and Zn-Ti mixed metal oxides. The photocatalytic process involving Zn-Ti MMOs, corresponding to a pseudo-first order reaction kinetic, proceeded in a diffusion mode with limiting step in the form of dye adsorption on the surface of photocatalyst. The photodegradation of MB in the presence of Zn-Ti LDH, which was more accurately described by a pseudo-second order model, occurred in a kinetic regime, where the photocatalytic reaction was the limiting stage.

Mixed metal oxides of zinc and titanium had significantly higher functional characteristics compared to their Zn-Ti LDH precursor. The calcination of Zn-Ti layered double hydroxide at 200–500 °C allowed to achieve the highest photocatalytic activity of Zn-Ti MMO, which was due to phase transformations occurring during thermal treatment. The decomposition of Zn-Ti LDH at 200–250 °C resulted in the formation of a crystalline phase of zinc oxide (ZnO), which had a hexagonal wurtzite crystal structure with the ability to effectively absorb radiation from almost the entire UV spectral region. The rise of the Zn-Ti LDH calcination temperature to 500 °C led to an increase in the crystallinity degree of ZnO.

Keywords: concretes, self-cleaning, photocatalysts, layered double hydroxides, synthesis, thermal treatment, mixed metal oxides, phase composition, ZnO, methylene blue, photodegradation, kinetic models

*Corresponding author E-mail: artbalrun@yandex.ru

Received October 12, 2024; Received in revised form November 20, 2024; Accepted February 12, 2025

Please cite this article as: Balykov A.S., Nizina T.A., Chugunov D.B., Davydova N.S., Kyashkin V.M. Photocatalysts based on Zn-Ti layered double hydroxide and its calcination products for self-cleaning concretes: Structure formation and photocatalytic activity. Construction Materials and Products. 2025. 8 (1). 2. DOI: 10.58224/2618-7183-2025-8-1-2

1. INTRODUCTION

The development of high performance cement materials is a priority direction of modern building materials science [1, 2]. It is known that individual or complex application of chemical and mineral additives with different composition and mechanism of action [3, 4] allows to create high performance concretes [5, 6]. A special group of modifiers includes photocatalytic additives [7, 8] that make it possible to obtain photocatalytically active cement systems [9, 10] characterized by a number of positive properties such as the ability to self-clean and decompose atmospheric pollutants, antibacterial effect, etc. [11, 12]. The use of such materials will allow to implement the main provisions of the green building concept, in particular, to improve the quality of atmospheric air in localities, to increase the level of architectural possibilities of the urban environment, etc. [13, 14].

Mixed transition metal oxides are one of the effective types of photocatalysts, because they have improved functional characteristics, including higher activity and resistance to deactivation compared to monometallic compounds [15, 16]. The synthesis of such composite metal oxide systems may involve thermal decomposition of various precursors, among which layered double hydroxides have high efficiency [17, 18].

Layered double hydroxides (LDHs) are a group of two-dimensional hydrotalcite-like materials consisting of positively charged mixed layers of metal hydroxide separated by water molecules and charge-balancing inorganic and organic anions of various compositions (CO_3^{2-}, SO_4^{2-}, NO_3^-, Cl^-, etc.) [19, 20]. Two or more types of divalent and trivalent/tetravalent metal ions (Zn^{2+}, Mg^{2+}, Cu^{2+}, Ni^{2+}, Fe^{3+}, Al^{3+}, Ti^{4+}, Sn^{4+}, etc.) are usually part of the hydroxide brucite-like layers of LDHs [21, 22]. Thus, layered double hydroxides and their calcination products are in demand photocatalytic materials due to their wide variety, possibility of targeted changes in properties and low cost [23, 24].

The purpose of this study was to establish the effects of synthesis conditions on the structure parameters and photocatalytic activity of zinc-titanium layered double hydroxide (Zn-Ti LDH) with Zn^{2+}/Ti^{4+} molar ratio of 2/1, as well as its calcination products in the form of zinc-titanium mixed metal oxides (Zn-Ti MMOs).

The following tasks were solved to achieve the aim of this study:

The effects of precipitation, aging, and drying parameters on the phase composition and size of crystallites (coherent scattering regions (CSR)) of Zn-Ti LDH were established.

The physico-chemical processes occurring during the thermal treatment of Zn-Ti LDH were studied.

The influence of Zn-Ti LDH calcination temperature on the phase composition and photocatalytic activity of Zn-Ti MMOs was revealed.

The interrelations and regularities were installed in the systems of ‘synthesis conditions – Zn-Ti LDH structure parameters’ and ‘Zn-Ti LDH calcination temperature – phase composition and photocatalytic activity of Zn-Ti MMO’, which allowed to optimize the prescription and technological parameters for obtaining effective photocatalysts for self-cleaning concretes.

2. METHODS AND MATERIALS

2.1. Synthesis of Zn-Ti LDH and Zn-Ti MMOs samples

Zn-Ti LDH samples were obtained by co-precipitation at constant pH. Compound precipitation occurred at low supersaturation, when the alkaline solution in the form of precipitator mixture of NaOH (2 M) and Na_2CO_3 (0.67 M) was slowly added to the aqueous solution of the precursor salts of $Zn(NO_3)_2 \cdot 6H_2O$ (0.67 M) and $TiCl_4$ (0.33 M) while maintaining the required pH of the reaction medium. The following stages were aging, filtering, washing and drying of the resulting precipitate.

During the experimental study, the variable parameters of synthesis were:

- temperature at mixing of solutions (during precipitation of LDH) (Tmixing) equaled to 20 °C, 45C, and 70 °C;
- pH of the reaction medium amounted to 8, 9, and 10;
- feed rate of the alkaline solution (v) equaled to 2.5 ml/min, 5 ml/min, and 10 ml/min;
- temperature of precipitate aging (Taging) amounted to 20 °C, 45 °C, and 70 °C;
- time of precipitate aging (taging) equaled to 0 h, 2 h, 4 h, and 24 h;
- temperature of precipitate drying (Tdrying) amounted to 70 °C and 110 °C.

The sample drying time (tdrying) was constant at 14 h.

Table 1 shows the numbering of the studied samples of zinc-titanium layered double hydroxides and the values of their variable synthesis parameters. The control sample was Zn-Ti LDH characterized by the following synthesis conditions: pH 9, v=5 ml/min, Tmixing=20 °C, Taging=20 °C, taging=4 h, and Tdrying=70 °C.

Table 1. List of Zn-Ti LDH samples obtained under different synthesis conditions.

Sample number	Parameters of solution mixing / LDH precipitation			Parameters of precipitate aging		Parameters of precipitate drying	
	pH	v, ml/min	Tmixing, °C	Taging, °C	taging, h	Tdrying, °C	tdrying, h
1 (control)	9	5	20	20	4	70	14
2	8	5	20	20	4	70	14
3	10	5	20	20	4	70	14
4	9	2.5	20	20	4	70	14
5	9	10	20	20	4	70	14
6	9	5	20	70	4	70	14
7	9	5	45	45	4	70	14
8	9	5	70	70	4	70	14
9	9	5	70	70	4	110	14
10	9	5	20	70	6	70	14
11	9	5	20	20	2	70	14
12	9	5	20	20	0	70	14

To obtain zinc-titanium heteroxide systems, the control sample of Zn-Ti LDH (No. 1, Table 1) was calcined at 200 °C, 500 °C, and 800 °C. The designations of the obtained samples were Zn-Ti MMO-200, Zn-Ti MMO-500, and Zn-Ti MMO-800, respectively.

2.2. Thermal analysis of Zn-Ti LDH sample

The physico-chemical processes occurring during the thermal treatment of zinc-titanium layered double hydroxide were studied using the synchronous thermal analysis (STA), when combining thermogravimetric and differential thermal analysis methods. The research object was control sample of Zn-Ti LDH (No. 1, Table 1). TGA/DSC1 thermogravimetric analyzer (Mettler Toledo AG, Switzerland) was used during the study. The sample heating was to 1000 °C in air, the temperature rise rate was 10 °C/min. The corresponding experimental TG, DTG, and DTA curves were obtained as the research results.

2.3. X-ray diffraction phase analysis of Zn-Ti LDH and Zn-Ti MMO samples

The structure parameters of Zn-Ti layered double hydroxides and Zn-Ti mixed metal oxides were investigated by X-ray diffraction phase analysis on the PANalytical Empyrean diffractometer (the Netherlands). Shooting was done in the geometry according to Bragg-Brentano (θ–2θ scanning mode, 2θ=5–75°) using CuKα radiation characterized by weighted average wavelength λ=1.54 Å. The phases were identified using the Crystallography Open Database (COD).

The crystallinity degree of the photocatalyst structure was estimated by the size of coherent scattering regions (CSR) of the main phases, in particular, hydrotalcite for Zn-Ti LDH and zinc oxide for Zn-Ti MMOs.

The sizes of CSR (crystallites) of these phases were determined by the most intensive diffraction peaks at 2θ=12.9° for Zn-Ti hydrotalcite and 2θ=36.2° for ZnO, using the classical Scherrer formula:

$$D = L_{cr} = \frac{K \cdot \lambda}{\beta \cdot \cos\frac{2\theta}{2}}, \quad (1)$$

where D (Lcr) is the size of crystallites (CSR) of the analyzed phase, Å;

K is the particle shape coefficient (Scherrer constant), K≈0.9–1.0;

λ is the wavelength of X-ray radiation, λ=1.54 Å;

β is the full width at half maximum (FWHM) for the most intensive diffraction peak of the analyzed phase, radians;

θ is the X-ray diffraction angle, radians.

2.4. Evaluation of photocatalytic activity of Zn-Ti LDH and Zn-Ti MMO samples

The photocatalytic activity of the obtained samples was studied in a model photochemical reaction of oxidative destruction of methylene blue (MB), when aqueous suspensions of 'MB solution – Zn-Ti LDH' and 'MB solution – Zn-Ti MMO' were exposed to low-intensity ultraviolet radiation.

The suspensions were prepared using 125 mg of Zn-Ti LDH / Zn-Ti MMO powder and 250 ml of MB solution with a concentration of 10 mg/l, i.e. the weight ratio of photocatalyst and dye was 50/1. To destroy large agglomerates and evenly distribute the dispersed phase particles in the solution, ultrasonic dispersion of samples was performed for 10 min on the Bandelin Sonorex ultrasonic bath. Next, ultraviolet light irradiated the solutions for two hours with constant stirring on a magnetic stirrer. Two 25 W 254 nm UV lamps were used as the radiation sources. Aliquots of the dye solution were taken at certain time intervals, in particular, after 15 min, 30 min, 60 min, 90 min, and 120 min from the start of UV exposure. The selected samples were centrifuged for 15 min at 4000 rpm to separate the photocatalyst powder from the solution. The optical density of the solution (concentration of methylene blue) was measured at 664 nm relative to distilled water using the Shimadzu UV-1800 spectrophotometer.

The formulas for calculating the residual relative concentration (ΔCt,, rel. units) and the photocatalytic decomposition degree ($\varphi_{\Delta C_t}$, %) of methylene blue were:

$$\Delta C_t = \frac{C_t}{C_0}, \quad (2)$$

$$\varphi_{\Delta C_t} = (1 - \Delta C_t) \cdot 100\% = \left(1 - \frac{C_t}{C_0}\right) \cdot 100\% = \left(\frac{C_0 - C_t}{C_0}\right) \cdot 100\%, \quad (3)$$

where Ct is the optical density of MB solution after exposure to UV radiation during time (t), rel. units (it characterizes the current dye concentration at time (t), mmol/l);

C0 is the initial optical density of MB solution, rel. units (it characterizes the initial dye concentration before UV irradiation (t0=0 min), mmol/l).

3. RESULTS AND DISCUSSION

3.1. Effects of synthesis conditions on the structure parameters of Zn-Ti LDH

Fig. 1 shows the diffraction pattern of the Zn-Ti LDH control sample (No. 1, see Table 1).

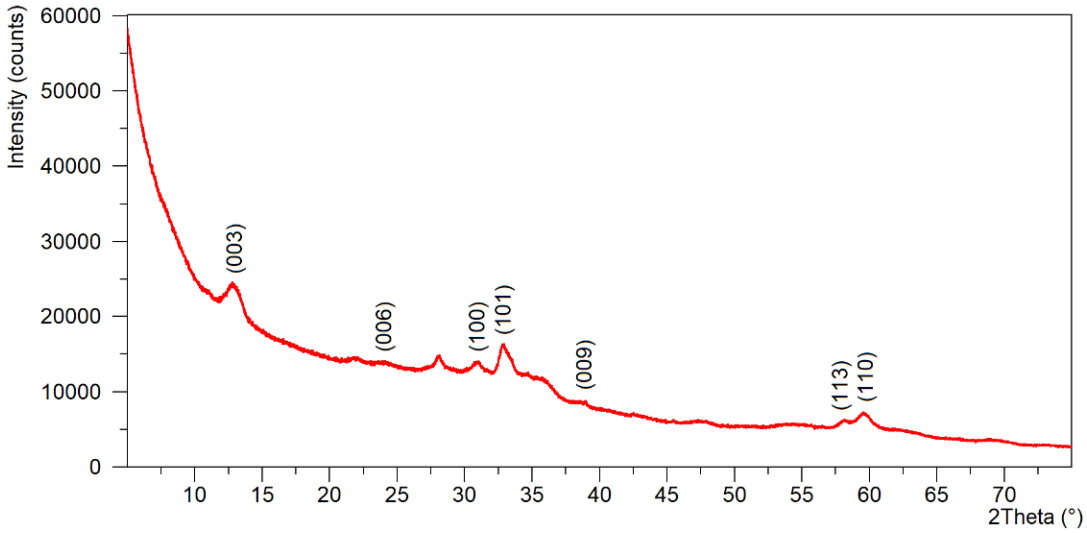

Fig. 1. Diffraction pattern of the Zn-Ti LDH control sample (No. 1, see Table 1).

The phase composition of the control sample (Figure 1) included zinc-titanium layered double hydroxide characterized by:

- the diffraction peaks located at 2θ003=12.9°, 2θ006=24.1°, and 2θ009=38.9° that corresponded to the (003), (006), and (009) basal reflection planes with d003=6.86 Å, d006=3.69 Å, and d009=2.31 Å;
- the diffraction peaks situated at 2θ100=30.9°, 2θ101=32.8°, 2θ113=58.0°, and 2θ110=59.6° associated with the (100), (101), (113), and (110) non-basal reflection planes with d100=2.89 Å, d101=2.73 Å, d113=1.59 Å, and d110=1.55 Å, respectively.

It is worth noting that the results obtained were in line with the previous studies, in particular [25, 26].

The experimental data in Table 2 showed:

X-ray diffraction patterns of samples synthesized at different pH showed peaks corresponding to the (003), (006), (100), (101), (009), (113), and (110) reflection planes of the Zn-Ti hydrotalcite lattice. For samples Nos. 1, 2, and 3, obtained at pH 9, pH 8, and pH 10, the crystallite sizes in the direction perpendicular to the (003) plane were 76 Å, 75 Å, and 77 Å, respectively. Thus, the change in the hydrogen index of the reaction medium in the considered range (pH of 8 to 10) did not significantly affect the crystallinity degree of the synthesized zinc-titanium layered double hydroxides.

Samples Nos. 1, 4, and 5 obtained at different feed rates of the alkaline solution were characterized by an identical phase composition represented by Zn-Ti hydrotalcite. Increasing the rate of solution supply of the precipitator mixture (NaOH + Na2CO3) from 2.5 ml/min to 10 ml/min led to a decrease in the coherent scattering region size in the direction normal to the (003) reflection plane from 78 Å to 67 Å. Thus, the growth of supersaturation in the reaction system, which intensifies the formation of crystallization nuclei, caused the decrease in the crystallinity degree of the synthesized Zn-Ti LDH samples at acceleration of alkaline solution supply.

Compared to the control sample No. 1, the increase in the precipitate aging temperature (Taging) from 20 °C to 70 °C for sample No. 6 led to the growth of the crystallite size from 76 Å to 84 Å without qualitative changes in the material mineralogical composition, which included one phase in the form of Zn-Ti hydrotalcite.

Analysis of changes in the structure characteristics of samples Nos. 7 and 8 relative to the control sample No. 1 showed that the simultaneous growth of the temperature at mixing of solutions (Tmixing) and temperature of precipitate aging (Taging) from 20 °C to 45 °C and 70 °C caused the rise in the Zn-Ti LDH crystallinity degree, in particular, the size of coherent scattering regions (CSR) in the direction normal to the (003) reflection plane increased from 76 Å to 78 Å and 85 Å, respectively (Table 2). At the same time, there were certain differences in the phase composition of the samples under study. In particular, compared with the samples Nos. 1 and 7, in sample No. 8 synthesized at the higher temperature (Tmixing=Taging=70 °C), along with hydrotalcite, there was the additional oxide phase in the form of ZnO.

Table 2. Phase composition and coherent scattering region size of Zn-Ti LDH samples obtained under different synthesis conditions.

Table 2. Phase composition and coherent scattering region size of Zn-Ty LDN samples obtained under different synthetic conditions.

Sample number	Phase composition	Size of coherent scattering regions in the direction normal to the (003) reflection plane (CSR003), Å
1 (control)	Zn-Ti hydrotalcite	76
2		75
3		77
4		78
5		67
6		84
7		78
8	Zn-Ti hydrotalcite and ZnO	85
9		87
10	Zn-Ti hydrotalcite	84
11		72
12		68

The comparative analysis results for the samples Nos. 8 and 9 indicated the slight increase in the crystallite size from 85 Å to 87 Å while maintaining the two-phase composition of the synthesized material (Zn-Ti hydrotalcite + ZnO) when the drying temperature (Tdrying) rose from 70 °C to 110 °C.

It was worth noting that the experimental data obtained were consistent with the known dependences describing the particle size enlargement with increasing temperature of layered double hydroxide synthesis, in particular [27]:

$$\frac{dL}{dt} = C \cdot e^{\left(\frac{-1}{R \cdot T}\right)}, \quad (4)$$

where L is the crystallite size (LDH particles);

t is the time of LDH synthesis;

$\frac{dL}{dt}$ is the rate of change in the LDH particle size over time;

C, R are constants;

T is the temperature of LDH synthesis.

The research results of the samples Nos. 1, 11, and 12 synthesized at Tmixing=Taging=20 °C and Tdrying=70 °C (Table 1), showed some reduction in the crystallinity degree of zinc-titanium layered double hydroxide when decreasing the precipitate aging time (taging) from 4 h to 0 h, in particular, the size of coherent scattering regions in the direction normal to the (003) reflection plane decreased from 76 Å to 68 Å (Table 2). In this case, increase in the precipitate aging time (taging) from 4 h to 6 h for samples Nos. 6 and 10 obtained at the higher precipitate aging temperature (Taging=70 °C) had no effect on the phase composition and crystallinity degree of Zn-Ti LDH.

3.2. Physico-chemical processes occurring during thermal treatment of Zn-Ti LDH

Fig. 2 shows the TG (1), DTG (2), and DTA (3) curves of the control sample of zinc-titanium layered double hydroxide (No. 1, see Table 1).

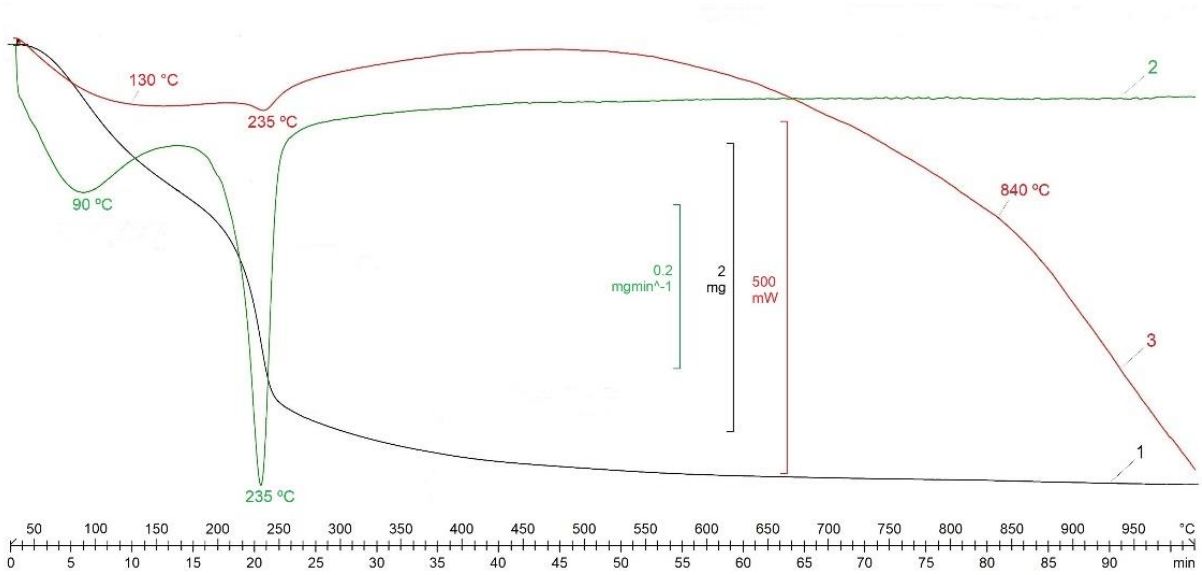

Fig. 2. TG (1), DTG (2), and DTA (3) curves of the Zn-Ti LDH control sample (No. 1, see Table 1).

It was found that the processes of dehydroxylation, decarbonization, and decomposition of Zn-Ti LDH occurred predominantly in the temperature range of 50–250 °C with the weight loss of about 17.6 wt. % (≈82 % of all weight losses according to the TG curve) and were carried out in two stages at 50–180 °C and 180–250 °C. A number of extrema on the DTA and DTG curves indicated this:

- wide endothermic effect in the temperature range of 50–180 °C with a maximum at 130 °C on the DTA curve characterized the initial stage of dehydration of Zn-Ti layered double hydroxide associated with the removal of interlayer and crystallization water from the sample. At this stage, Zn-Ti LDH lost 7.6 wt. % (≈35 % of all weight losses according to the TG curve), while the highest rate of sample dehydration occurred at 90 °C, as evidenced by the corresponding peak on the DTG curve;

- noticeable endothermic effect with a maximum at 235 °C was present on the DTA curve in the temperature range of 180–250 °C. This endothermic effect corresponded to the main stage of the Zn-Ti LDH decomposition process, characterized by the removal of interlayer carbonate anions and destruction of the crystal lattice of layered double hydroxide. According to the TG curve, the weight loss of Zn-Ti LDH at 180–250 °C was 10 wt. % (≈47 % of all weight losses), while the decomposition process of the sample was most intense at 235 °C (see DTG curve).

It was revealed that further temperature increase in the range of 250–1000 °C led to the completion of the Zn-Ti LDH decomposition process with the formation and crystallization of zinc-titanium mixed metal oxides (Zn-Ti MMOs). At this stage of calcination, the investigated sample lost 3.9 wt. %, which was approximately 18 % of the total weight losses. The Zn-Ti MMO crystallization was completed at 800–870 °C, as evidenced by the exothermic effect with a peak at 840 °C on the DTA curve.

3.3. Effect of calcination temperature on the phase composition of Zn-Ti MMOs

Figure 3 shows the diffraction patterns of Zn-Ti MMO-200, Zn-Ti MMO-500, and Zn-Ti MMO-800 mixed metal oxides obtained by calcination of Zn-Ti LDH (No. 1, see Table 1) at 200 °C, 500 °C, and 800 °C, respectively.

It was identified that the phase composition of Zn-Ti MMO-200 and Zn-Ti MMO-500 samples included predominantly individual oxide phases such as zinc oxide (ZnO) and titanium (IV) oxide (TiO2). The crystalline phase of ZnO with a hexagonal wurtzite structure was characterized by the diffraction peaks located at 2θ100=31.7°, 2θ002=34.3°, 2θ101=36.2°, 2θ102=47.5°, 2θ110=56.5°, 2θ103=62.8°, and 2θ112=67.9° that corresponded to the (100) (002), (101), (102), (110), (103), and (112) reflection planes with d100=2.82 Å, d002=2.61 Å, d101=2.48 Å, d102=1.91 Å, d110=1.63 Å, d103=1.48 Å, and d112=1.38 Å, respectively (Fig. 3). The TiO2 phase was in the X-ray amorphous state, as evidenced by the halo (broad blurry peak) at 2θ=25–40°.

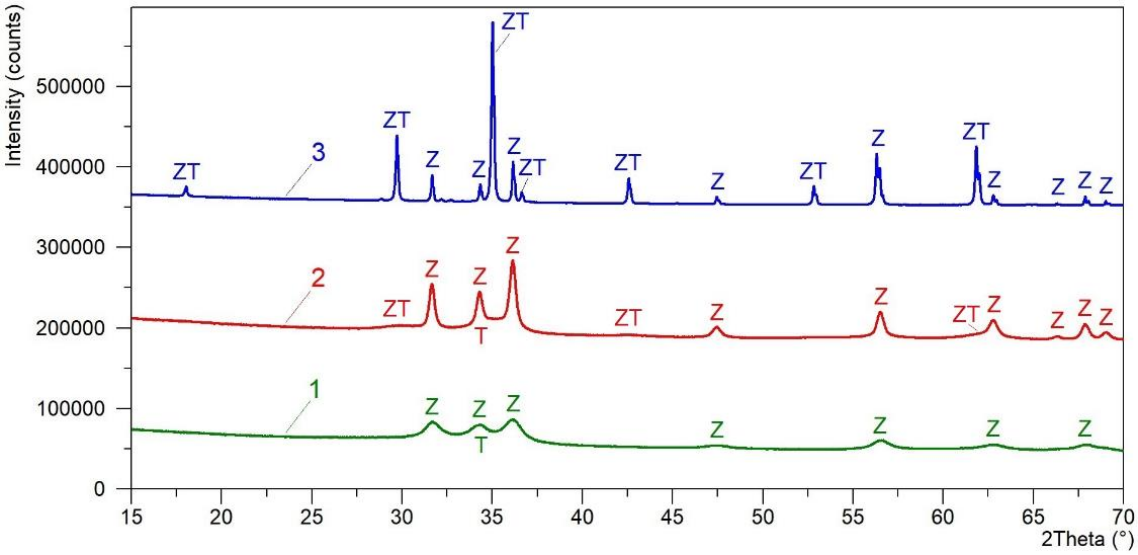

Fig. 3. Diffraction patterns of Zn-Ti MMO-200 (1), Zn-Ti MMO-500 (2), and Zn-Ti MMO-800 (3) samples with designated peaks of ZnO (Z), Zn2TiO4 (ZT), and X-ray amorphous TiO2 (T).

The mineralogical composition of the Zn-Ti MMO-800 sample synthesized at 800 °C included two crystalline phases represented by zinc oxide (ZnO) and zinc orthotitanate (Zn2TiO4). The Zn2TiO4 heterooxide phase with a spinel structure characterized by crystals with a cubic lattice exhibited the diffraction peaks situated at 2θ of 18.0°, 29.7°, 35.0°, 36.6°, 42.6°, 52.8°, and 61.8°, which corresponded to the d-spacing values of 4.92 Å, 3.01 Å, 2.56 Å, 2.45 Å, 2.12 Å, 1.73 Å, and 1.50 Å, respectively. It was worth noting that the diffraction pattern of the Zn-Ti MMO-500 sample also contained several small blurred peaks of Zn2TiO4 spinel, in particular, located at 2θ of 29.7°, 42.6°, and 61.8° with the d-spacing values of 3.01 Å, 2.12 Å, and 1.50 Å, respectively.

Thus, the results of the X-ray diffraction phase analysis of zinc-titanium mixed metal oxides corresponded to the thermal analysis data presented in paragraph 3.2, as well as with the results of studies by other authors, in particular [25, 26]. The thermal decomposition of Zn-Ti layered double hydroxide at 200–250 °C resulted in the formation of two individual oxide phases in the form of X-ray amorphous TiO2 and crystalline ZnO with a hexagonal wurtzite structure. The rise of the Zn-Ti LDH calcination temperature to 500 °C led to an increase in the crystallinity degree of ZnO and initiated the formation of additional phase of Zn2TiO4 with the cubic spinel structure. The crystallization of ZnO/Zn2TiO4 heteroxide system was completed at 800–870 °C.

The ZnO phase, present in all studied samples, was a marker of the growth of the structure crystallinity degree in the Zn-Ti MMO-200, Zn-Ti MMO-500, Zn-Ti MMO-800 row when the synthesis temperature of zinc-titanium mixed metal oxides increased. In particular, the recorded FWHM values for the most intensive diffraction peak of ZnO at 2θ101=36.2° (with d101=2.48 Å) showed an increase in the crystallite (CSR) size of this phase in the direction normal to the (101) reflection plane from 114 Å to 588 Å (i.e., 5.2 times) when the calcination temperature of Zn-Ti LDH rose from 200 °C to 800 °C.

3.4. Photocatalytic activity of Zn-Ti LDH and Zn-Ti MMOs

It is known [28] that the rate of a dye solution discoloration during photocatalysis is determined by the combined action of several basic processes, such as:

1. Dye photodegradation in the liquid phase.
2. Dye adsorption on the photocatalyst surface.
3. Photocatalytic decomposition of dye molecules adsorbed on the surface of photocatalyst particles.

Processes 2 and 3 are sequential, while the dye photodegradation in the liquid phase proceeds independently and simultaneously with processes 2 and 3.

It is worth to dwell separately on the mechanism of the dye photodecomposition process No. 3 with the participation of semiconductor photocatalysts, such as zinc oxide (ZnO), titanium (IV) oxide

(TiO2), and ZnO/Zn2TiO4 mixed metal oxides. At the first stage, the semiconductor absorbs a photon with a (hv) energy exceeding the band gap energy of the photocatalyst, which leads to the generation of an electron-hole pair. At the second stage there are diffusion processes of generated charge carriers to the crystallite surface, while some of charge carriers recombine in the volume and on the surface of semiconductor, which reduces the quantum yield of the photocatalytic process. In the third step, the free electron and hole react with water and molecular oxygen adsorbed on the photocatalyst particle surface, which leads to the formation of the •OH hydroxyl radical and the $\bullet O_2^-$ superoxide anion radical. These radicals are highly active and enter into redox reactions with pollutants to form simple inorganic ions and compounds such as CO2, H2O, NH4+, NO3−, SO42−, etc. [29, 30].

Fig. 4 shows the photodegradation kinetic curves of methylene blue (MB) in solution under exposure conditions of ultraviolet radiation in the absence and presence of Zn-Ti LDH, Zn-Ti MMO-200, Zn-Ti MMO-500, and Zn-Ti MMO-800 photocatalysts. The kinetic curves show the change in relative dye concentration in solution (ΔCt), calculated by the formula (2), during UV irradiation for 120 min.

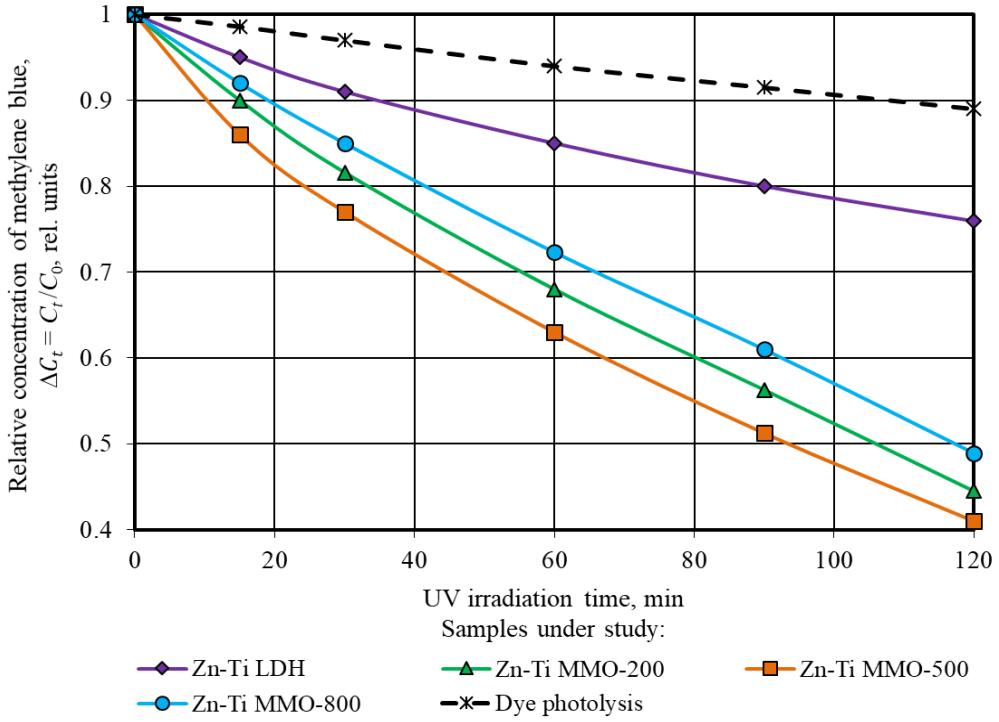

Fig. 4. Kinetic curves of methylene blue photodegradation in solution under UV radiation in the absence of photocatalysts (black dotted curve characterizes to MB photolysis) and in the presence of Zn-Ti layered double hydroxide or Zn-Ti mixed metal oxides (colored solid curves characterize to MB photocatalytic decomposition processes).

It was found that the concentration of methylene blue in the solution decreased exponentially under ultraviolet exposure. The highest rate of photochemical reaction of dye decomposition was observed in the first 15–30 minutes of UV light irradiation (Fig. 4). The MB decomposition degree in solution ($\varphi_{\Delta C_t}$, see formula (3)) in the absence of photocatalyst was $\varphi_{\Delta C_{120\ min}}$=11 % after 120 min of UV exposure. When using Zn-Ti LDH powder, the $\varphi_{\Delta C_{120\ min}}$ parameter value increased 2.2 times to a level of 24 %. The presence of photocatalysts based on zinc-titanium mixed metal oxides in the solution significantly improved the efficiency of dye photodegradation. In particular, for Zn-Ti MMO-200, Zn-Ti MMO-500, and Zn-Ti MMO-800 samples the decrease in the concentration of methylene blue after 120 min of UV irradiation was 56 %, 59 %, and 51 % (Fig. 4). This was 4.6–5.4 times and 2.1–2.5 times higher than the $\varphi_{\Delta C_{120\ min}}$ values recorded during the photolysis of MB in solution

without photocatalyst and during the photocatalytic decomposition of dye in the presence of Zn-Ti LDH, respectively.

It is known that the Langmuir–Hinshelwood kinetic model is widely used to describe the kinetics of photolysis and photocatalytic degradation of dye molecules in an aqueous medium, while experimental data are usually approximated by linearized integral forms of pseudo-first (5) or pseudo-second (6) order reaction equations [31, 32]:

$$-\ln(\frac{C_t}{C_0}) = k_1 \cdot t, \quad (5)$$

$$\frac{1}{C_t} - \frac{1}{C_0} = k_2 \cdot t, \quad (6)$$

where C0 and Ct are the initial and current concentrations of the dye in aqueous solution (the same as in formulas (2) and (3)), mmol/l;

t is the time of photochemical reaction, such as photolysis or photocatalytic degradation of the dye, characterized by the duration of UV irradiation, min;

k1 is the rate constant of photochemical reaction, such as photolysis or photocatalytic decomposition of the dye, in the linearized pseudo-first order kinetic equation (5), min-1;

k2 is the rate constant of photochemical reaction, such as photolysis or photocatalytic decomposition of the dye, in the linearized pseudo-second order kinetic equation (6), l/(mmol·min).

Fig. 5 shows graphs describing the kinetics of photolysis and photocatalytic decomposition of methylene blue in solution under UV light irradiation by pseudo-first order (a) and pseudo-second order (b) reaction equations. The angle of inclination of the linear dependences made it possible to determine the rate constant values of the corresponding photochemical reactions occurring in the absence and in the presence of photocatalysts.

It was found that the presence of Zn-Ti LDH and Zn-Ti MMOs in the solution significantly accelerated the methylene blue decomposition process upon UV light irradiation. The rate constant values of the corresponding photocatalytic reactions when used the pseudo-first order and pseudo-second order kinetic models were k1=0.0024–0.0075 min-1 and k2=0.088–0.3582 l/(mmol·min), which were 2.4–7.5 times and 3.9–15.9 times higher than those for dye photolysis without photocatalysts (k1=0.001 min-1 and k2=0.0225 l/(mmol·min)).

The calcination products of zinc-titanium layered double hydroxide, such as Zn-Ti MMO-200, Zn-Ti MMO-500, and Zn-Ti MMO-800, had significantly higher photocatalytic activity compared to their Zn-Ti LDH precursor. In particular, the rate constant values of the pseudo-first order and pseudo-second order reactions of methylene blue photodecomposition in the presence of Zn-Ti MMOs were k1=0.0057–0.0075 min-1 and k2=0.2496–0.3582 l/(mmol·min) (Fig. 5). It was 2.4–3.1 times and 2.8–4.1 times higher than the corresponding kinetic parameters of k1=0.0024 min-1 and k2=0.088 l/(mmol·min) characterized by the photocatalytic process of dye degradation with the participation of Zn-Ti LDH. The identified features of the phase composition of zinc-titanium mixed metal oxides, in particular, the presence of crystalline phase of ZnO with a hexagonal wurtzite structure (see paragraph 3.3), possessing the ability to effectively absorb radiation from almost the entire UV spectral region, resulted in higher functional characteristics of Zn-Ti MMO photocatalysts.

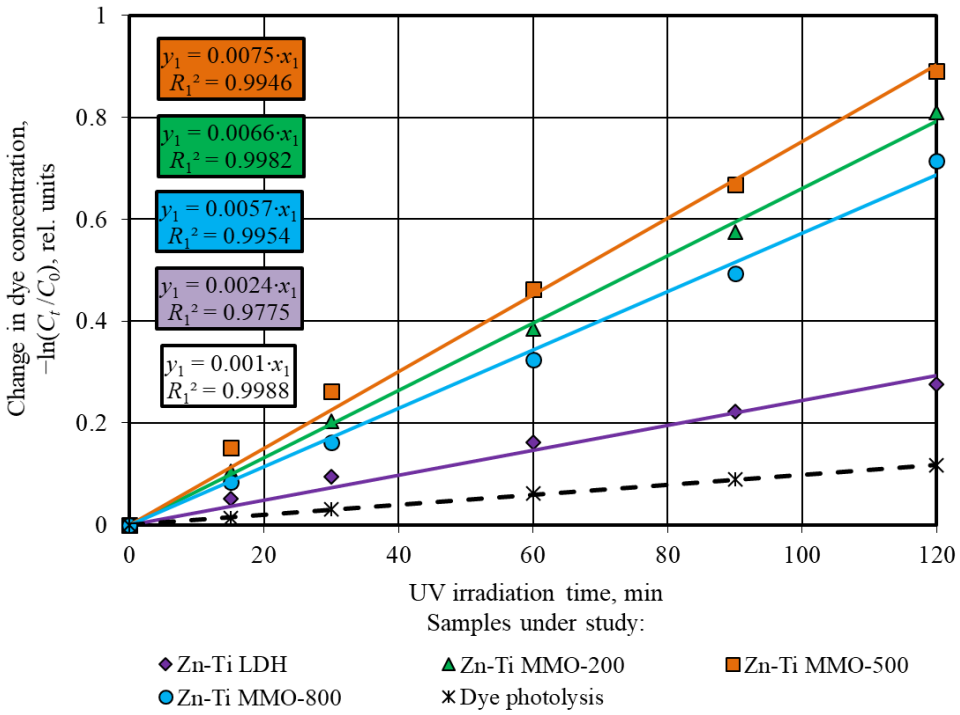

(a)

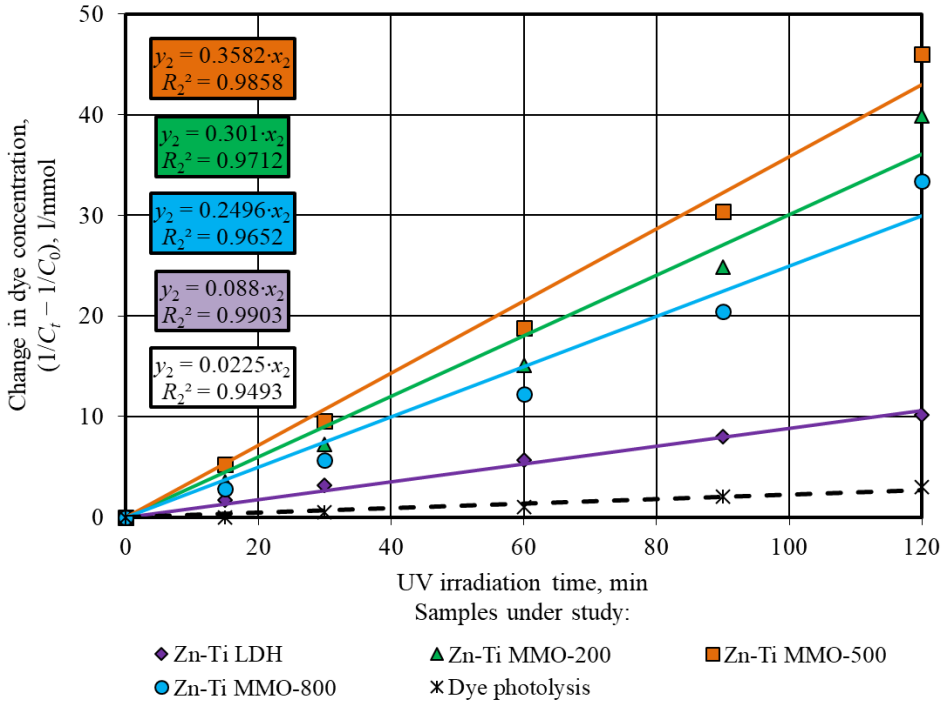

(b)

Fig. 5. Description of the methylene blue photodegradation kinetics in solution under UV radiation in the absence (black dotted lines) and in the presence of photocatalysts (colored solid lines) in the coordinates of pseudo-first order (a) and pseudo-second order (b) kinetic models.

It was identified that the photocatalytic activity of zinc-titanium mixed metal oxide samples increased in the Zn-Ti MMO-800, Zn-Ti MMO-200, Zn-Ti MMO-500 direction (Figs. 4 and 5). The functional characteristics of Zn-Ti MMO decreased when the synthesis temperature rises from 200–500 °C to 800 °C due to the concentration reduction of the most photoactive phase of ZnO through the formation of additional heteroxide phase of Zn_2TiO_4 in the photocatalyst structure. At the same time, in comparison with Zn-Ti MMO-500, some decrease in the photocatalytic reaction rate with the participation of Zn-Ti MMO-200 could be due to the lower degree of its structure crystallinity. In particular, the FWHM values for the most intensive diffraction peak of ZnO at $2\theta_{101}=36.2°$ (see Fig. 3) showed reduced in the crystallite (CSR) size of this phase in the direction normal to the (101) reflection plane from 249 Å to 114 Å (i.e., 2.2 times) when the calcination temperature of Zn-Ti LDH decreased from 500 °C to 200 °C.

The experimental data obtained during the study of photochemical reactions under UV radiation were satisfactorily approximated by the pseudo-first order (5) and pseudo-second order (6) equations, as evidenced by high values of the corresponding determination coefficients of R1=0.9775–0.9988 and R2=0.9493–0.9903. It was recorded that the kinetics of the methylene blue photocatalytic decomposition processes in the presence of zinc-titanium mixed metal oxides (Zn-Ti MMOs), as well as the dye photolysis without the participation of photocatalysts, were most adequately described by the pseudo-first order kinetic model, because R1=0,9946–0,9988 > R2=0,9493–0,9858. At the same time, the kinetics of the MB photodegradation reaction involving Zn-Ti layered double hydroxide was better described by the pseudo-second order kinetic model (R2=0.9903 > R1=0.9775) (Fig. 5).

It is known [32, 33] that heterogeneous reactions have two possible modes of course depending on the limiting stage, in particular, kinetic and diffusion modes characterized by the limiting contribution of chemical reaction or diffusion, respectively. A more accurate description of the experimental data by the pseudo-second order kinetic model indicates the limiting contribution of the chemical reaction to the heterogeneous process. The correspondence of the process kinetics to the pseudo-first order model suggests that the diffusion stage limits the heterogeneous reaction.

Thus, the previously noted distinctive features of the photochemical reaction kinetics involving Zn-Ti LDH and Zn-Ti MMOs indicated differences in their course mode. The photodegradation of methylene blue in solution under UV irradiation in the presence of Zn-Ti layered double hydroxide occurred in the kinetic regime with the limiting contribution of the photocatalytic reaction, because the pseudo-second order model (6) described the kinetics of this process more adequately. The MB photodestruction with the participation of zinc-titanium mixed metal oxides, corresponding to the pseudo-first order reaction kinetic (5), occurred in the diffusion regime, in which the dye adsorption on the Zn-Ti MMO surface was the limiting stage.

4. CONCLUSIONS

The following scientific results were obtained in the paper:

The effects of precipitation, aging, and drying parameters on the phase composition and size of crystallites (coherent scattering regions) of Zn-Ti layered double hydroxide were established.

The physico-chemical processes occurring during the thermal treatment of Zn-Ti LDH were disclosed.

The influence of Zn-Ti LDH calcination temperature on the phase composition and photocatalytic activity of zinc-titanium mixed metal oxides was revealed.

The interrelations and regularities were installed in the systems of ‘synthesis conditions – Zn-Ti LDH structure parameters’ and ‘Zn-Ti LDH calcination temperature – phase composition and photocatalytic activity of Zn-Ti MMO’, which allowed to optimize the prescription and technological parameters for obtaining effective photocatalysts for self-cleaning concretes.

The research results showed differences in the kinetics of photodestruction of methylene blue in solution under UV radiation in the presence of Zn-Ti layered double hydroxide and Zn-Ti mixed metal oxides. The photocatalytic process involving Zn-Ti MMOs, corresponding to a pseudo-first order reaction kinetic, proceeded in a diffusion mode with limiting step in the form of dye adsorption on the surface of photocatalyst. The photodegradation of MB in the presence of Zn-Ti LDH, which was more

accurately described by a pseudo-second order model, occurred in a kinetic regime, where the photocatalytic reaction was the limiting stage.

Mixed metal oxides of zinc and titanium had significantly higher functional characteristics compared to their Zn-Ti LDH precursor. The calcination of Zn-Ti layered double hydroxide at 200–500 °C allowed to achieve the highest photocatalytic activity of Zn-Ti MMO, which was due to phase transformations occurring during thermal treatment. The decomposition of Zn-Ti LDH at 200–250 °C resulted in the formation of a crystalline phase of zinc oxide (ZnO), which had a hexagonal wurtzite crystal structure with the ability to effectively absorb radiation from almost the entire UV spectral region. The rise of the Zn-Ti LDH calcination temperature to 500 °C led to an increase in the crystallinity degree of ZnO.

5. ACKNOWLEDGMENTS

The research was supported by grant from the Russian Science Foundation (project No. 23-79-01029), https://rscf.ru/en/project/23-79-01029/

REFERENCES

[1] Khan K., Johari M.A.M., Amin M.N., Nasir M. Development and evaluation of basaltic volcanic ash based high performance concrete incorporating metakaolin, micro and nano-silica. Developments in the Built Environment. 2024. 17. Art. no. 100330. https://doi.org/10.1016/j.dibe.2024.100330

[2] Tayeh B.A., Akeed M.H., Qaidi S., Bakar B.H.A. Ultra-high-performance concrete: Impacts of steel fibre shape and content on flowability, compressive strength and modulus of rupture. Case Studies in Construction Materials. 2022. 17. Art. no. e01615. https://doi.org/10.1016/j.cscm.2022.e01615

[3] Klyuev S., Fediuk R., Ageeva M., Fomina E., Klyuev A., Shorstova E., Zolotareva S., Shchekina N., Shapovalova A., Sabitov L. Phase formation of mortar using technogenic fibrous materials. Case Studies in Construction Materials. 2022. 16. P. e01099.

[4] Nizina T.A., Balykov A.S., Korovkin D.I., Volodin V.V. Physical and mechanical properties of modified fine-grained fibre-reinforced concretes containing carbon nanostructures. International Journal of Nanotechnology. 2019. 16. P. 496 – 509. https://doi.org/10.1504/IJNT.2019.106621

[5] Fediuk R., Amran M., Klyuev S., Klyuev A. Increasing the performance of a fiber-reinforced concrete for protective facilities. Fibers. 2021. 9 (11). Art. no. 64. https://doi.org/10.3390/fib9110064

[6] Balykov A.S., Nizina T.A., Volodin S.V. Optimization of technological parameters for obtaining mineral additives based on calcined clays and carbonate rocks for cement systems. Nanotechnologies in Construction. 2022. 14 (2). P. 145 – 155. https://doi.org/10.15828/2075-8545-2022-14-2-145-155

[7] Klyuev S., Fediuk R., Ageeva M., Fomina E., Klyuev A., Shorstova E., Sabitov L., Radaykin O., Anciferov S., Kikalishvili D., de Azevedo Afonso R.G., Vatin N. Technogenic fiber wastes for optimizing concrete. Materials. 2022. 15 (14). P. 5058.

[8] Balykov A.S., Nizina T.A., Kyashkin V.M., Volodin S.V. Evaluation of the effectiveness of mineral additives in cement systems in the development of “core – shell” photocatalytic compositions. Nanotechnologies in Construction. 2022. 14 (5). P. 405 – 418. https://doi.org/10.15828/2075-8545-2022-14-5-405-418

[9] Amor F., Baudys M., Racova Z., Scheinherrová L., Ingrisova L., Hajek P. Contribution of TiO_2 and ZnO nanoparticles to the hydration of Portland cement and photocatalytic properties of High Performance Concrete. Case Studies in Construction Materials. 2022. 16. Art. no. e00965. https://doi.org/10.1016/j.cscm.2022.e00965

[10] Balykov A.S., Nizina T.A., Kyashkin V.M., Chugunov D.B. Siliceous rocks as modifiers of structure of photocatalytic self-cleaning concrete. Impact assessment on phase composition of cement stone. Nanotechnologies in Construction. 2024. 16 (2). P. 158 – 169. https://doi.org/10.15828/2075-8545-2024-16-2-158-169

[11] Janczarek M., Klapiszewski Ł., Jędrzejczak P., Klapiszewska I., Ślosarczyk A., Jesionowski T. Progress of functionalized TiO_2-based nanomaterials in the construction industry: A comprehensive review. Chemical Engineering Journal. 2022. 430 (3). Art. no. 132062. https://doi.org/10.1016/j.cej.2021.132062

[12] Yang L., Hakki A., Wang F., Macphee D.E. Photocatalyst efficiencies in concrete technology: The effect of photocatalyst placement. Applied Catalysis B: Environmental. 2018. 222. P. 200 – 208. https://doi.org/10.1016/j.apcatb.2017.10.013

[13] Amran M., Fediuk R., Klyuev S., Qader D.N. Sustainable development of basalt fiber-reinforced high-strength eco-friendly concrete with a modified composite binder. Case Studies in Construction Materials. 2022. 17. e01550.

[14] Klyuev S., Klyuev A., Fediuk R., Ageeva M., Fomina E., Amran M., Murali G. Fresh and mechanical properties of low-cement mortars for 3D printing. Construction and Building Materials. 2022. № 338. P. 127644. DOI:10.1016/j.conbuildmat.2022.127644

[15] Janani F.Z., Khiar H., Taoufik N., Elhalil A., Sadiq M., Puga A.V., Mansouri S., Barka N. $ZnO–Al_2O_3–CeO_2–Ce_2O_3$ mixed metal oxides as a promising photocatalyst for methyl orange photocatalytic degradation. Materials Today Chemistry. 2021. 21. Art. no. 100495. https://doi.org/10.1016/j.mtchem.2021.100495

[16] Al Miad A., Saikat S.P., Alam Md.K., Hossain Md. S., Bahadur N.M., Ahmed S. Metal oxide-based photocatalysts for the efficient degradation of organic pollutants for a sustainable environment: a review. Nanoscale Advances. 2024. 6 (19). P. 4781 – 4803. https://doi.org/10.1039/d4na00517a

[17] Peng D., Zhang Y. Engineering of mixed metal oxides photocatalysts derived from transition-metal-based layered double hydroxide towards selective oxidation of cyclohexane under visible light. Applied Catalysis A: General. 2023. 653. Art. no. 119067. https://doi.org/10.1016/j.apcata.2023.119067

[18] Jiménez A., Trujillano R., Rives V., Vicente M.A. Mixed–metal–oxide photocatalysts generated by high–temperature calcination of CaAlFe, hydrocalumite–LDHs prepared from an aluminum salt–cake. Catalysis Today. 2023. 423. Art. no. 114008. https://doi.org/10.1016/j.cattod.2023.01.015

[19] Boumeriame H., Da Silva E.S., Cherevan A.S. Layered double hydroxide (LDH)-based materials: A mini-review on strategies to improve the performance for photocatalytic water splitting. Journal of Energy Chemistry. 2022. 64. P. 406 – 431. https://doi.org/10.1016/j.jechem.2021.04.050

[20] Yang Z.Z., Zhang C., Zeng G.M., Tan X.F., Huang D.L., Zhou J.W., Fang Q.Z., Yang K.H., Wang H., Wei J., Nie K. State-of-the-art progress in the rational design of layered double hydroxide based photocatalysts for photocatalytic and photoelectrochemical H_2/O_2 production. Coordination Chemistry Reviews. 2021. 446. Art. no. 214103. https://doi.org/10.1016/j.ccr.2021.214103

[21] Taoufik N., Sadiq M., Abdennouri M., Qourzal S., Khataee A., Sillanpää M., Barka N. Recent advances in the synthesis and environmental catalytic applications of layered double hydroxides-based materials for degradation of emerging pollutants through advanced oxidation processes. Materials Research Bulletin. 2022. 154. Art. no. 111924. https://doi.org/10.1016/j.materresbull.2022.111924

[22] Seftel E.M., Niarchos M., Vordos N., Nolan J.W., Mertens M., Mitropoulos A.Ch., Vansant E.F., Cool P. LDH and TiO_2/LDH-type nanocomposite systems: A systematic study on structural characteristics. Microporous and Mesoporous Materials. 2015. 203. P. 208 – 215. https://doi.org/10.1016/j.micromeso.2014.10.029

[23] Ludvíková J., Jirátová K., Kovanda F. Mixed oxides of transition metals as catalysts for total ethanol oxidation. Chemical Papers. 2012. 66 (6). P. 589 – 597. https://doi.org/10.2478/s11696-011-0127-x

[24] Al-Aani H.M.S., Trandafir M.M., Fechete I., Leonat L.N., Badea M., Negrilă C., Popescu I., Florea M., Marcu, I.-C. Highly Active Transition Metal-Promoted CuCeMgAlO Mixed Oxide Catalysts Obtained from Multicationic LDH Precursors for the Total Oxidation of Methane. Catalysts. 2020. 10 (6). Art. no. 613. https://doi.org/10.3390/catal10060613

[25] Puscasu C.M., Seftel E.M., Mertens M., Cool P., Carja G. ZnTiLDH and the Derived Mixed Oxides as Mesoporous Nanoarchitectonics with Photocatalytic Capabilities. Journal of Inorganic and Organometallic Polymers and Materials. 2015. 25. P. 259 – 266. https://doi.org/10.1007/s10904-014-0132-y

[26] Sahu R.K., Mohanta B.S., Das N.N. Synthesis, characterization and photocatalytic activity of mixed oxides derived from ZnAlTi ternary layered double hydroxides. Journal of Physics and Chemistry of Solids. 2013. 74 (9). P. 1263 – 1270. https://doi.org/10.1016/j.jpcs.2013.04.002

[27] Bukhtiyarova M.V., Bulavchenko O.A., Bukhtiyarov A.V., Nuzhdin A.L., Bukhtiyarova G.A. Selective Hydrogenation of 5-Acetoxymethylfurfural over Cu-Based Catalysts in a Flow Reactor: Effect of Cu-Al Layered Double Hydroxides Synthesis Conditions on Catalytic Properties. Catalysts. 2022. 12 (8). Art. no. 878. https://doi.org/10.3390/catal12080878

[28] Bulyga D.V., Evstropiev S.K. Kinetics of adsorption and photocatalytic decomposition of a diazo dye by nanocomposite ZnO–MgO. Optics and Spectroscopy. 2022. 130 (9). P. 1176. https://doi.org/10.21883/eos.2022.09.54839.3617-22

[29] Syuleiman Sh.A., Yakushova N.D., Pronin I.A., Kaneva N.V., Bojinova A.S., Papazova K.I., Gancheva M.N., Dimitrov D.Tz., Averin I.A., Terukov E.I., Moshnikov V.A. Study of the photodegradation of brilliant green on mechanically activated powders of zinc oxide. Technical Physics. 2017. 62 (11). P. 1709 – 1713. https://doi.org/10.1134/S1063784217110287

[30] Man H., Wen C., Luo W., Bian J., Wang W., Li C. Simultaneous deSO_x and deNO_x of marine vessels flue gas on ZnO-CuO/rGO: Photocatalytic oxidation kinetics. Journal of Industrial and Engineering Chemistry. 2020. 92. P. 77 – 87. https://doi.org/10.1016/j.jiec.2020.08.022

[31] Fatimah I., Yahya A., Iqbal R.M., Tamyiz M., Doong R.-a., Sagadevan S., Oh W.-C. Enhanced Photocatalytic Activity of Zn-Al Layered Double Hydroxides for Methyl Violet and Peat Water Photooxidation. Nanomaterials. 2022. 12 (10). Art. no. 1650. https://doi.org/10.3390/nano12101650

[32] Irani M., Mohammadi T., Mohebbi S. Photocatalytic Degradation of Methylene Blue with ZnO Nanoparticles; a Joint Experimental and Theoretical Study. Journal of the Mexican Chemical Society. 2016. 60 (4). P. 218 – 225.

[33] Khamizov R.Kh. A Pseudo-Second Order Kinetic Equation for Sorption Processes. Russian Journal of Physical Chemistry A. 2020. 94 (1). P. 171 – 176. https://doi.org/10.1134/S0036024420010148

INFORMATION ABOUT THE AUTHORS

Balykov A.S., artbalrun@yandex.ru, ORCID ID: https://orcid.org/0000-0001-9087-1608, SCOPUS: https://www.scopus.com/authid/detail.uri?authorId=57190170885, National Research Mordovia State University, Candidate of Engineering Sciences (Ph.D.), Associate Professor of Building Constructions Department

Nizina T.A., nizinata@yandex.ru, ORCID ID: https://orcid.org/0000-0002-2328-6238, SCOPUS: https://www.scopus.com/authid/detail.uri?authorId=57190161363, National Research Mordovia State University, Doctor of Engineering Sciences (Advanced Doctor), Professor of Building Constructions Department

Chugunov D.B., iman081@gmail.com, ORCID ID: https://orcid.org/0000-0002-1612-0539, SCOPUS: https://www.scopus.com/authid/detail.uri?authorId=56453268900, National Research Mordovia State University, Candidate of Chemical Sciences (Ph.D.), Associate Professor of Inorganic and Analytical Chemistry Department

Davydova N.S., davydowanatalia@yandex.ru, ORCID ID: https://orcid.org/0009-0008-9409-682X, National Research Mordovia State University, Laboratory Assistant at Research Laboratory of Ecological and Meteorological Monitoring, Building Technologies and Expertises

Kyashkin V.M., kyashkin@mail.ru, ORCID ID: https://orcid.org/0000-0002-3413-247X, SCOPUS: https://www.scopus.com/authid/detail.uri?authorId=7801669853, National Research Mordovia State University, Candidate of Physico-Mathematical Sciences (Ph.D.), Associate Professor of Physical Materials Science Department